RUNX1 cooperates with FLT3–ITD to induce leukemia

Kira Behrens,[1] Katrin Maul,[1] Nilgün Tekin,[1,2] Neele Kriebitzsch,[1] Daniela Indenbirken,[3] Vladimir Prassolov,[4] Ursula Müller,[1] Hubert Serve,[5] Jörg Cammenga,[6] and Carol Stocking[1]

[1]Retroviral Pathogenesis, [2]Virus Genomics, and [3]Viral Transformation, Heinrich-Pette-Institute, Leibniz Institute for Experimental Virology, 20251 Hamburg, Germany
[4]Engelhardt Institute for Molecular Biology, 119991 Moscow, Russia
[5]Department of Medicine, Hematology/Oncology, Johann Wolfgang Goethe-University, 60590 Frankfurt am Main, Germany
[6]Department of Hematology, Institute for Clinical and Experimental Medicine, Linköping University, 58185 Linköping, Sweden

Acute myeloid leukemia (AML) is induced by the cooperative action of deregulated genes that perturb self-renewal, proliferation, and differentiation. Internal tandem duplications (ITDs) in the FLT3 receptor tyrosine kinase are common mutations in AML, confer poor prognosis, and stimulate myeloproliferation. AML patient samples with FLT3-ITD express high levels of RUNX1, a transcription factor with known tumor-suppressor function. In this study, to understand this paradox, we investigated the impact of RUNX1 and FLT3-ITD coexpression. FLT3-ITD directly impacts on RUNX1 activity, whereby up-regulated and phosphorylated RUNX1 cooperates with FLT3-ITD to induce AML. Inactivating RUNX1 in tumors releases the differentiation block and down-regulates genes controlling ribosome biogenesis. We identified *Hhex* as a direct target of RUNX1 and FLT3-ITD stimulation and confirmed high *HHEX* expression in FLT3-ITD AMLs. HHEX could replace RUNX1 in cooperating with FLT3-ITD to induce AML. These results establish and elucidate the unanticipated oncogenic function of RUNX1 in AML. We predict that blocking RUNX1 activity will greatly enhance current therapeutic approaches using FLT3 inhibitors.

INTRODUCTION

Acute myeloid leukemia (AML) is a clinically heterogeneous group of cancers caused by genetic and epigenetic alterations that cumulatively drive aberrant proliferation and block differentiation of hematopoietic stem and progenitor cells (HSPCs). Cytogenetic and molecular studies have identified several genes that are affected by recurrent somatic mutations in different AML subtypes. This information has led to a greater understanding of AML biology, allowed better risk stratification to guide therapeutic strategies, and provided new targets for drug development (Marcucci et al., 2011; Cancer Genome Atlas Research Network, 2013; Sanders and Valk, 2013). Nevertheless, long-term survival rates for AML remain dismally poor, with relapse being the most frequent cause of therapeutic failure in leukemia (Burnett et al., 2011; Patel et al., 2012). Understanding the intracellular interactions of driver mutations with secondary changes that propel leukemia progression (e.g., block differentiation) and/or confer drug resistance is essential to improve therapeutic outcomes.

One of the most frequent mutations in AML is internal tandem duplication (ITD) of the *FLT3* gene, leading to

constitutive activation of FLT3 receptor tyrosine (Tyr) kinase (Stirewalt and Radich, 2003; Small, 2006). Although FLT3 mutations do not define a distinct disease entity, they are of high prognostic relevance with strong association with reduced overall survival (Small, 2006; Patel et al., 2012). Analysis of remission clones has demonstrated a high retention frequency of FLT3-ITD mutations and the acquisition of homozygous mutant alleles (uniparental disomy), suggesting that FLT3-ITD signaling provides a key selective advantage to the cancer and to drug resistance (Thiede et al., 2002; Gale et al., 2008; Paguirigan et al., 2015). FLT3-ITD mutations are often secondary to initiating mutations that confer self-renewal properties to the founder clone, such as mutations in DNMT3A, RUNX1, or TET2 (Welch et al., 2012; Genovese et al., 2014; Shlush et al., 2014). Thus, activated FLT3 likely promotes the expansion of a preleukemic clone that subsequently incurs a block in differentiation, the hallmark of acute leukemia. Mouse models support the impact of FLT3-ITD in the induction of abnormal myeloproliferation and have also demonstrated that, alone, it is insufficient to induce acute leukemia (Grundler et al., 2005; Lee et al., 2007; Chu et al., 2012). It is currently unresolved what genetic or epigenetic events are responsible for the profound block in differentiation in AML and whether shared genetic programs acting downstream of FLT3-ITD signaling contribute to this block. An appealing hypothesis is that
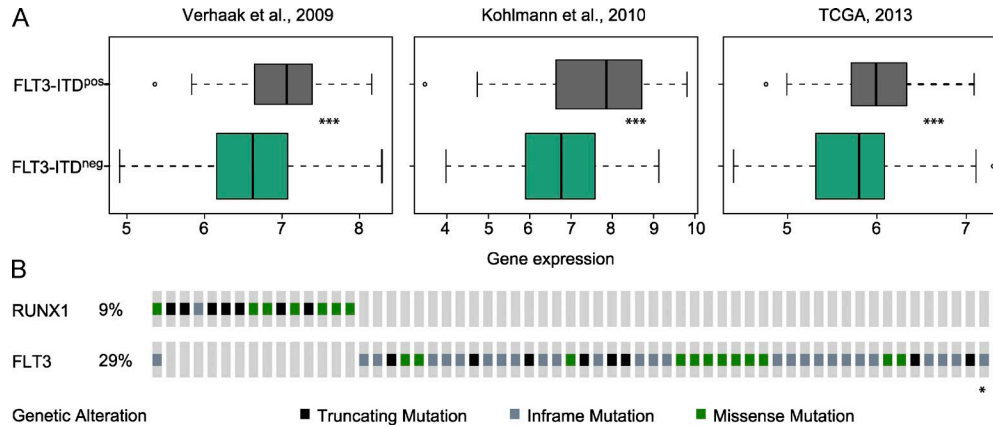
Figure 1. **RUNX1 gene expression levels and mutation frequency in FLT3–ITD[pos] leukemia.** (A) Relative *RUNX1* expression levels (log2) of AML samples from three independent studies calculated using the Leukemia Gene Atlas. P-values were calculated with Welch's *t* test. ***, P < 0.001. TCGA, the Cancer Genome Atlas Research Network (2013). (B) Activating FLT3 mutations and inactivating RUNX1 mutations significantly tend toward mutual exclusivity. Diagram and statistics were generated with the National Cancer Institute Genomic Data Commons cBioPortal using the Cancer Genome Atlas AML databank. *n* = 191. *, P < 0.05.

FLT3-ITD signaling either directly or indirectly impacts the transcriptional circuitry that controls differentiation decisions.

RUNX1 encodes a key transcriptional regulator of hematopoiesis and thus, not surprisingly, is a frequent target of chromosomal translocations and inactivating mutations in both myeloid and lymphoid neoplasms (Niebuhr et al., 2008; Grossmann et al., 2011; Lam and Zhang, 2012). *Runx1* inactivation in mouse models has demonstrated critical functions in several blood lineages: maturation of megakaryocytes (Meg), initiation and progression of B cell development, and stage-specific development of T cells (Ichikawa et al., 2004; Collins et al., 2009; Wong et al., 2011b; Niebuhr et al., 2013). In addition, Runx1 has been implicated in the inhibition of self-renewal programs in early HSPCs (Growney et al., 2005; Ross et al., 2012; Lam et al., 2014; Behrens et al., 2016). This latter function likely explains its known tumor suppressor activity, mirrored in the high incidence of inactivating mutations (10–20%) in AML (Osato et al., 1999; Schnittger et al., 2011; Cancer Genome Atlas Research Network, 2013). Early studies have also demonstrated the interplay of RUNX1 with several granulocyte/macrophage (G/M) transcription factors (TFs; e.g., C/EBP, PU.1, and GFI1) during normal myelopoiesis (Rosenbauer and Tenen, 2007), and thus, a popular theory is that reduced levels of RUNX1 activity contributes to the myeloid differentiation block in AML.

During analysis of gene expression patterns within several large AML patient cohorts available through the Leukemia Gene Atlas (Hebestreit et al., 2012), we observed a consistent and significant increase in *RUNX1* transcript levels in FLT3-ITD[pos] samples (Fig. 1 A). Furthermore, *RUNX1* inactivation mutations were significantly underrepresented in FLT3-ITD[pos] AMLs (Fig. 1 B). Thus, we sought to investigate whether high levels of RUNX1 contribute to AML induc-

tion and to explore the interaction between FLT3-ITD mutations and RUNX1 activity.

RESULTS

RUNX1 and FLT3–ITD synergize to induce AML with high penetrance and short latency

To test the hypothesis that increased levels of RUNX1 and FLT3-ITD cooperate to induce AML, we established a retroviral transduction/transplantation mouse model (Fig. 2 A). Overexpression of RUNX1 is known to prevent efficient transplantation of HSPCs (Challen and Goodell, 2010). Thus, a vector expressing RUNX1-ERt2 was generated in which RUNX1 activity (RUNX1*) can be induced with 4-hydroxytamoxifen (4-OHT). HSPCs isolated from B6.*Runx1*[Δ/+] mice were cotransduced with two retroviral vectors, one expressing RUNX1-ERt2 coupled with GFP and the other expressing FLT3-ITD and blue fluorescent protein (BFP). Using this protocol, 6–20% double-positive GFP[+]/BFP[+] HSPCs were obtained (Fig. 2 B). Transplanted mice receiving 4-OHT (+RUNX1*) developed a severe hematopoietic malignancy with an extremely short latency and with close to 100% penetrance (Fig. 2 C). Untreated transplanted mice (−RUNX1*) also developed a hematopoietic abnormality but with <50% penetrance, slower latency, and distinct characteristics.

Based on several clinical, cytohistological, and immunophenotypical criteria, the disease that developed in mice of the RUNX1*/FLT3-ITD cohorts could be classified as AML, in contrast to the myeloproliferative neoplasm (MPN) developing in mice with FLT3-ITD and nonactivated RUNX1. Both AML and MPN mice presented with lethargy, shortness of breath, splenomegaly, anemia, and leukocytosis, although leukocyte counts were higher in the MPN cohort (Fig. 2, D and E). Hepatomegaly as well as extensive and diffuse pulmonary infiltrations were restricted to AML in RUNX1*/
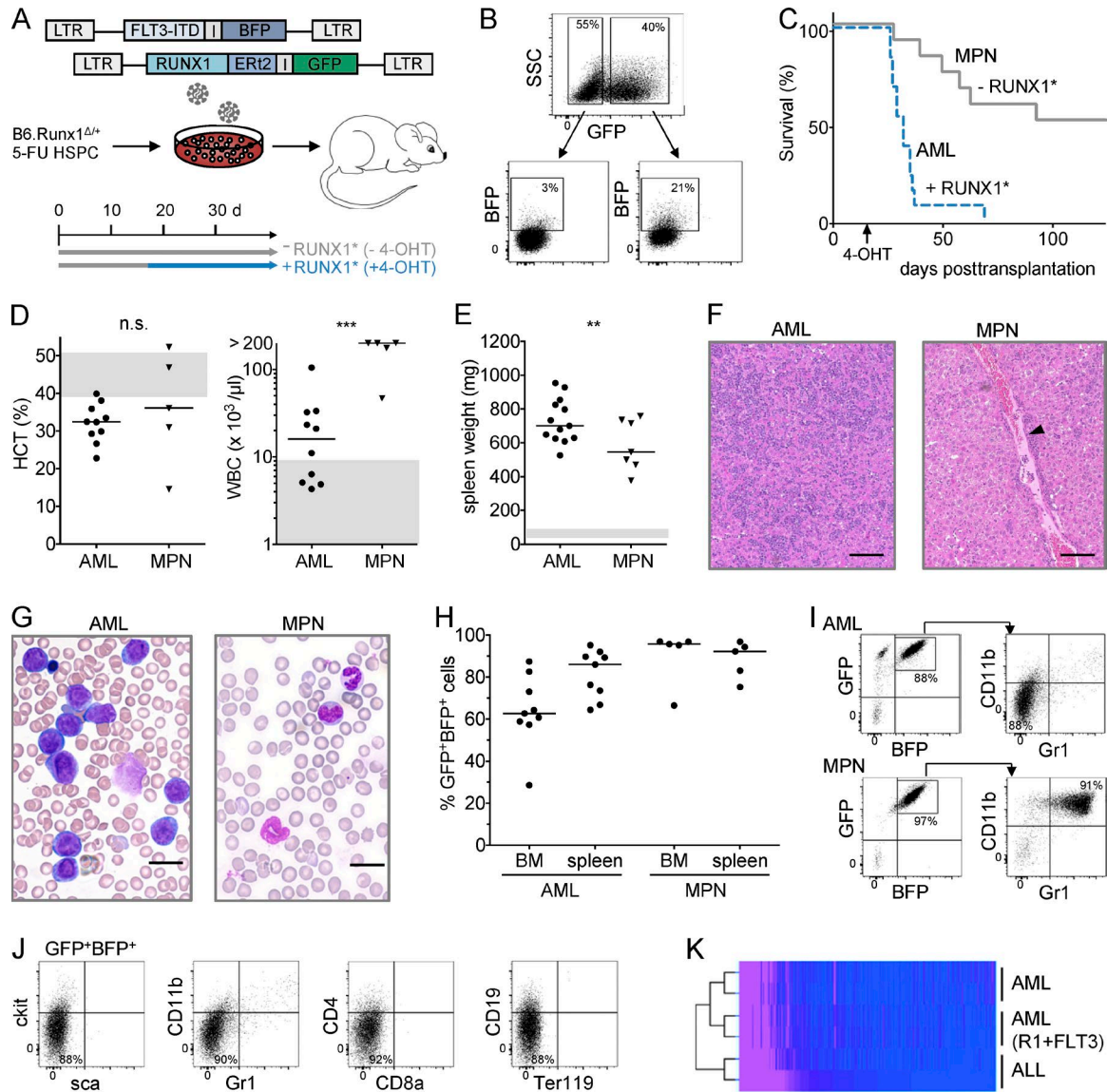
Figure 2. FLT3–ITD cooperates with high RUNX1 levels to induce a minimally differentiated AML. (A) Schematic representation of the experimental design. HSPCs were isolated from 5-FU–treated B6.$Runx1^{\Delta/+}$ mice, transduced with retroviral vectors, and transplanted into conditioned recipient mice. Half of the transplanted mice were administered 4-OHT–impregnated pellets from day 18 onwards. (B) Representative flow cytometry of HSPCs before transplantation demonstrating co-transduction. The titers of FLT3-ITD/BFP viral particles were lower than that of RUNX1-ERt2/GFP[+], but a skewing toward double-positive cells was observed, consistent with increased infection susceptibility of highly proliferating cells. In three independent experiments, 5.8, 11.3, or 21% of the GFP[+] population was transduced with the BFP vector. SSC, side scatter. (C) Kaplan-Meier survival curves of mice from the +RUNX1* cohort (4-OHT treated; n = 13) or -RUNX1* cohort (untreated; n = 12) from three independent experiments. (D) Blood analysis of diseased mice receiving 4-OHT (RUNX1*) and developing an AML (dots; n = 10) or from the untreated cohort developing an MPN (inverted triangles; n = 5). Hematocrit (HCT) values and white blood cell (WBC) counts are plotted for each individual mouse. Gray shading shows the range of normal values in age-matched controls. Horizontal lines show median values. P-values were calculated by a nonpaired Student's t test. (E) Spleen weight of diseased mice developing AML (dots; n = 13) or MPN (inverted triangle; n = 7). **, P < 0.01; ***, P < 0.001. (F) Representative histological analysis of livers isolated from either AML (4-OHT; n = 3) or MPN (uninduced; n = 3) mice. Abundant and diffuse infiltrating hematopoietic cells (dark staining) were observed in livers of AML mice, in contrast to the small focal infiltrations in portal tracts and sinusoids in MPN mice (arrowhead). H&E staining was used. Bars, 300 μm. (G) Blood smears demonstrating homogenous blast morphology of proliferating cells in AML mice (n = 3), opposed to the mature phenotype of proliferating cells in MPN mice (n = 3). The heterochromatic erythrocytes reflect the moderate anemia observed in both mouse cohorts. Pappenheim stain was used. Bars, 20 μm. (H) Dot blot showing the high percentage of double-positive (GFP[+]/BFP^{+}) cells in BM and spleen of AML (n = 9) or MPN (n = 5) mice. Each dot represents the value for a single mouse. Horizontal lines indicate median value. (I) Representative flow cytometry analysis of BM cells demonstrating high levels of GFP[+]/BFP^{+} cells and differential expression of CD11b/Gr1 myeloid antigens. Whereas, on average, 86.5 ± 12.4% of GFP^{+}/BFP^{+} cells from MPN mice (n = 5) were CD11b^{+}/Gr1^{+}, only 9.5 ± 5.4% from AML mice (n = 9) were positive for these myeloid markers. (J) Representative flow cytometry analyses of BM cells isolated from AML mice

FLT3-ITD mice, with MPN mice showing only restricted small focal portal and sinusoidal infiltrates (Fig. 2 F and Fig. S1). Examination of the hypercellular BM sections and blood films confirmed a homogenous population of blast cells in AML mice, in contrast to the increased levels of mature G/M in MPN mice (Figs. 2 G and Fig. S1).

Surface markers and gene expression analysis were used to confirm AML and MPN diagnosis. BM and splenic cells of diseased mice from both 4-OHT–treated (AML) and untreated (MPN) cohorts contained high levels of GFP$^+$/BFP$^+$ cells (Fig. 2 H). However, whereas the MPN cells expressed both Gr1 and CD11b antigens (typical of mature myeloid cells and a myeloproliferation), AML cells were negative for both myeloid markers (Fig. 2 I). AML cells were also negative for the myeloid progenitor marker kit as well as markers for B, T, and erythroid (Ery) cells (Fig. 2 J). Gene expression data obtained from the leukemic cells was compared with that from neoplastic cells from either (a) a pro–B cell acute lymphoblastic leukemia (ALL; induced with FLT3-ITD) or (b) an AML (induced with the RUNX1/RUNX1t1 fusion protein) by unsupervised clustering, confirming closer relatedness with the AML samples (Fig. 2 K). Furthermore, we could confirm expression of genes encoding TFs typically expressed in early myeloid cells (Cebpa, Gata2, and Gfi1b; Fig. S2). The AML phenotype in all RUNX1*/FLT-ITD mice was highly reproducible in a total of six independent experiments.

The distinct AML phenotype induced by activation of RUNX1 in conjunction with FLT3-ITD expression, as opposed to the expansion phenotype (myeloproliferation) in FLT3-ITD cells without activated RUNX1, demonstrates the synergistic action of these two events. However, to determine the influence of the B6.$Runx1^{\Delta/+}$ genotype of the donor cells to the disease phenotype, the experiment was performed using B6.$Runx1^{+/+}$ as well as B6.$Runx1^{\Delta/\Delta}$ HSPCs. Again, induction of AML was exclusively observed in the activated RUNX1 cohorts (i.e., 4-OHT treated) in both genetic backgrounds, although the latency was prolonged and incidence decreased in the B6.$Runx1^{+/+}$ background (Fig. 3). This somewhat contradictory result is likely caused by the increased self-renewal capacity of myeloid HSPCs in B6.$Runx1^{\Delta/\Delta}$ and B6.$Runx1^{\Delta/+}$ backgrounds, resulting in an initial expansion of transduced cells (Growney et al., 2005; Behrens et al., 2016). This would increase the probability of a differentiation-blocked subpopulation emerging after activation of transduced RUNX1. Collectively, this analysis demonstrates an oncogenic activity of RUNX1 in cooperation with FLT3-ITD and also supports an independent tumor suppressor activity of Runx1 in leukemia initiation.

RUNX1 activity is essential for RUNX1*/FLT3–ITD–induced leukemia and its maintenance

To test whether activated RUNX1 is necessary to both initiate and drive disease progression, we evaluated the effect of removing 4-OHT after RUNX1 induction for 5 d (pulse; Fig. 4 A). Transduction frequencies of B6.$Runx1^{\Delta/+}$ HSPCs were comparable with previous experiments (Fig. 4 B). Peripheral blood (PB) samples were taken weekly to monitor the expansion of GFP$^+$/BFP$^+$ cells (Fig. 4 C). At day 28 after transplantation, the percentage of GFP$^+$/BFP$^+$ cells was similar in both cohorts, but whereas 82% of the +RUNX1* mice developed AML by day 35, 83% of the mice receiving the 4-OHT pulse remained free of hematopoietic disease during a 100-d observation period (Fig. 4 D). Although only one animal in the pulse cohort developed fatal MPN disease, the majority of mice analyzed at the last time point presented with splenomegaly (Fig. 4 E). These results are consistent with the conclusion that maintenance of RUNX1 activation is necessary for the conversion of FLT3-ITD–induced MPN to AML.

To further investigate the importance of RUNX1 in disease maintenance, primary tumor cells were transplanted into conditioned recipients that were subjected to 4-OHT at day 0 or day 11 or left untreated (Fig. 4 F). Strikingly, whereas >80% of the transplanted mice treated at day 11 developed AML within 50 d, untreated mice remained healthy for >150 d (Fig. 4 G). Consistent with the negative impact of RUNX1 expression on transplantation efficiencies, mice receiving 4-OHT starting at day 0 failed to develop AML. Serial transplantations of the leukemic cells resulted in selection of variants that were capable of inducing AML with 100% penetrance in <25 d (Fig. 4 H). Together, these results demonstrate that RUNX1* together with FLT3-ITD induces a transplantable acute leukemia and, furthermore, that the expression of RUNX1 is necessary for maintenance of the disease.

Posttranslational modifications of RUNX1 are critical for stability and oncogenic activity

To investigate whether FLT3-ITD signaling impacts on RUNX1 activity in AML, we examined human AML cell lines reported to express FLT3-ITD. Consistent with our observation that RUNX1 transcript levels are higher in FLT3-ITD$^+$ AML samples, we observed high RUNX1 protein levels in the FLT3-ITD$^+$ cell line MV4;11. Only moderate levels of RUNX1 protein were observed in Molm13 cells, which carry but do not express the FLT3-ITD allele (Quentmeier et al., 2003), and K562 cells, which express the constitutive active BCR/ABL fusion kinase but do not exhibit FLT3 mutations (Fig. 5 A). Interestingly, expression levels of RUNX1-ER in AML cells isolated from our FLT3-ITD

(gated on GFP$^+$/BFP$^+$ cells) to investigate the expression of myeloid and lymphoid antigens. n = 10. (K) Unsupervised cluster analysis of the transcriptomes of neoplastic BM cells isolated from mice with AML induced with either RUNX1*/FLT3-ITD$^+$ (AML; R1 + FLT3) or RUNX1/RUNX1t1 (AML; not depicted) or from mice with a pro–B cell ALL induced with FLT3-ITD alone (expressing CD43$^+$CD19$^+$; not depicted). For each leukemia type, two samples derived from independent mice were sequenced. Relative expression levels (pink, high; blue, low) of individual genes (n = 41,882) are plotted for each leukemic sample.
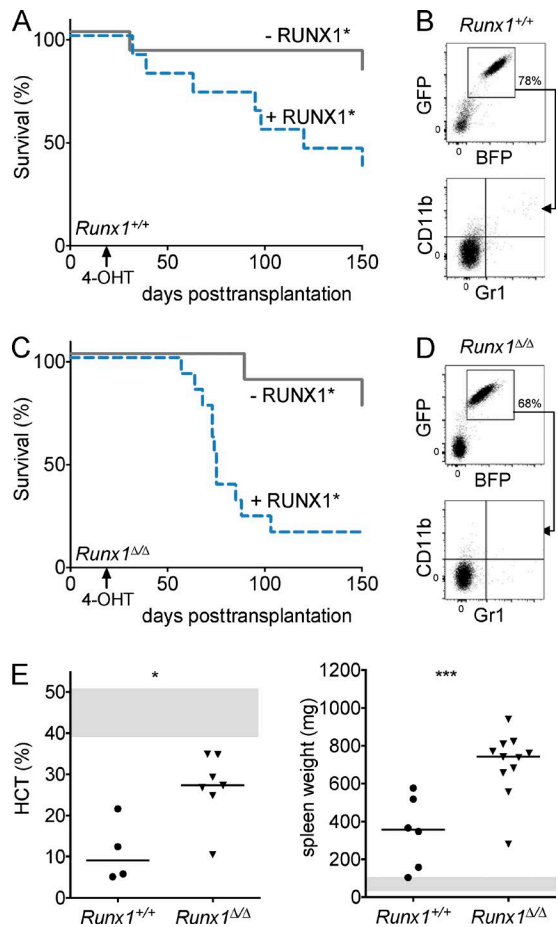
Figure 3. **Runx1–deficient genetic background accelerates AML induction.** (A) The Kaplan-Meier survival curves for mice transplanted with B6.*Runx1*^{+/+} HSPCs transduced with FLT3-ITD and RUNX1-ERt2 and either left untreated (−RUNX1*; *n* = 11) or treated with 4-OHT (+RUNX1*; *n* = 11). Results are from three independent experiments. (B) Representative flow cytometry plots of *B6.Runx1*^{+/+} BM cells isolated from diseased mice in the RUNX1* cohort demonstrating double-positive cells (median = 59.3%; *n* = 8) and which lacked mature myeloid markers. (C) Kaplan-Meier survival curves of mice transplanted with transduced *B6.Runx1*[Δ/Δ] HSPCs and either left untreated (−RUNX1*; *n* = 8) or treated with 4-OHT (+RUNX1*; *n* = 13). Results are from three independent experiments. (D) Representative flow cytometry plots of *B6.Runx1*[Δ/Δ] BM cells isolated from sick mice in the +RUNX1* cohort, confirming double-positive cells (median = 58%; *n* = 7), which lack mature myeloid markers. (E) Blood hematocrit (HCT) values and spleen weights of AML mice originating from either *B6.Runx1*^{+/+} or *B6.Runx1*[Δ/Δ] HSPCs in the +RUNX1* cohorts. Gray shading shows the range of normal values in age-matched controls. Horizontal lines show median values. P-values were calculated by a nonpaired Student's *t* test. *, P < 0.05; ***, P < 0.001.

mouse models were similarly high as RUNX1 in MV4;11 cells (Fig. 5 B), although this finding needs to be strengthened by examining protein levels in primary AML cells. Strikingly, RUNX1 protein levels in MV4;11 cells were greatly reduced after 24-h treatment with FLT3 inhibitors but not with a MAPK inhibitor (Fig. 5 C). As RUNX1 stability/activity is highly dependent on phosphorylation (Goyama et al., 2015), we generated phosphorylation mutants in which residues targeted by downstream effectors of FLT3-ITD (e.g., MAPK or Src kinases) were altered (Fig. 5 D). Disruption of either Tyr or Ser/Thr phosphorylation sites within the negative regulatory DNA-binding domain of RUNX1 did not impact on RUNX1 sensitivity to Sunitinib treatment in FLT3-ITD–expressing cells. In contrast, mutants with disrupted Tyr phosphorylation sites within the inhibitory domain (ID) lost sensitivity to Sunitinib inhibition, suggesting these residues may be critical for FLT3-ITD–mediated activation of RUNX1 (Fig. 5 E).

To test more rigorously the impact of RUNX1 phosphorylation and its transforming activity in cooperation with FLT3-ITD, the RUNX1 phosphorylation mutants were tested in our in vivo model. In agreement with a critical role of Tyr phosphorylation within the ID domain, all mutants except the ID mutant induced a fatal AML (Fig. 5 F), despite comparable transduction levels and transplantation efficiencies of all constructs, as determined by flow cytometry analysis of PB cells (Fig. 5 G). Collectively, we identified key phosphorylation sites in RUNX1 that mediate its transforming activity in collaboration with FLT3-ITD.

High levels of RUNX1 are critical for maintenance of established human AML cells

To begin to assess whether our results obtained in a mouse system could be transferred to human AML, we asked whether decreasing the high levels of RUNX1 in MV4;11 cells by shRNA technology would impact on tumor formation in a xenograft mouse model. Two shRNAs were identified that, when expressed via a lentiviral vector coexpressing the Venus fluorescent protein, resulted in reduced RUNX1 protein levels (Fig. 6, A and B). Transduced MV4;11 cells with reduced RUNX1 levels showed a growth disadvantage in vitro using competition assays (Fig. 6 C). Finally, in contrast to control-transduced MV4;11 cells, shRNA-RUNX1–transduced cells failed to induce rapid, fatal tumorigenic growth in vivo (Fig. 6, D and E). It is unlikely that this effect is mediated by defective homing of shRNA-RUNX1 cells, as first, consistent with another study (Cai et al., 2011), we have not observed reduced homing in HSPCs lacking Runx1 (unpublished data), and second, CXCR4 expression levels were not reduced in MV4;11 cells expressing shRNA-RUNX1 (Fig. 6 F). Collectively, these results demonstrate the critical role of RUNX1 levels in the tumorigenic growth of FLT3-ITD AML.

Identification of RUNX1 target genes that block myeloid differentiation

In view of the critical role of activated RUNX1 in orchestrating the switch from an MPN phenotype to AML, we sought to identify critical RUNX1 target genes. AML cells with either a *B6.Runx1*[Δ/+] or *B6.Runx1*[Δ/Δ] background were isolated from diseased mice and split into two cultures with or without 4-OHT. GFP[+]/BFP^{+} cells were sorted and used for
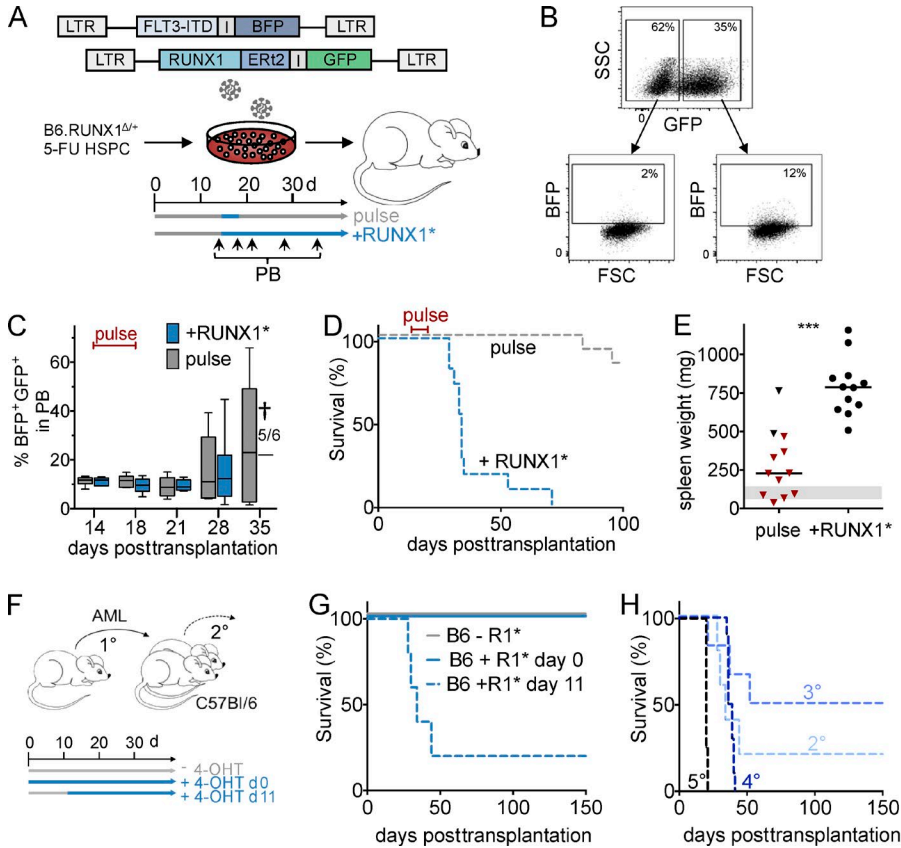
Figure 4. **RUNX1 is necessary for initiation and maintenance of FLT3–ITD–induced AML.** (A) Schematic representation of the experimental design. Half of the transplanted mice were administered 4-OHT at day 14 for 5 d (pulse cohort). Arrows indicate time points at which PB was analyzed. (B) Representative flow cytometry plots of transduced HSPCs before transplantation demonstrating double-transduced cells. Two independent experiments were performed with 12.1 or 10.3% of the GFP⁺ population transduced with the BFP vector. FSC, forward scatter; SSC, side scatter. (C) Two-dimensional box plots showing mean (line), 25–75th percentiles (boxed), and SD (whiskers) of GFP⁺/BFP⁺ cells in PB of transplanted mice (*n* = 6) at the indicated time points. By day 35, five out of six mice in the +RUNX1* cohort had developed AML. (D) Combined Kaplan-Meier survival curves of mice from either the pulse (*n* = 12) or continuous (*n* = 11) cohorts from two independent experiments. (E) Spleen weight of each mouse determined either when animals showed clear signs of disease (black symbols; *n* = 14) or at the termination of the experiment at day 100 (red inverted triangles; *n* = 10). Horizontal lines show median values. Gray horizontal bars show normal spleen weights of control mice. P-values were calculated by a nonpaired Student's *t* test. ***, P < 0.001. (F) Experimental setup for serial transplantation of AML cells.

Transplanted mice were divided into three cohorts and either given 4-OHT–impregnated feed starting at day 0 or 11 or left untreated. The experiment was repeated four times using donor mice from three independent experiments. Transplanted cells were derived from either spleen or BM and had a median GFP⁺/BFP⁺ population of 74%. *n* = 4. (G) Combined Kaplan-Meier survival curves of mice from either the untreated (*n* = 8), the day 0–treated (*n* = 14), or the day 11–treated (*n* = 5) cohort from two independent experiments. (H) Kaplan-Meier survival curves of serial transplantation of RUNX1*/FLT3-ITD⁺ leukemic blasts (*n* ≥ 4 per transplantation). All transplanted mice were treated with 4-OHT starting at day 11.

transcriptome analysis. A total of 221 genes were significantly differentially expressed by greater than a factor of two in both experiments (Fig. 7 A). STRING analysis in combination with gene ontology (GO) term enrichment analysis was used to identify biological networks that reflect the deregulated genes (Fig. 7 B). Inactivating RUNX1 resulted in the striking up-regulation of genes implicated in Meg/Ery differentiation but also genes identified as regulators of innate immunity, which are predominantly expressed in mature G/M cells. These results are consistent with a critical role of RUNX1 in maintaining a block in myeloid differentiation. Consistently, down-regulated genes revealed a preponderance of factors involved in ribosome biogenesis, indicative of differentiating cells that are no longer proliferating (Wong et al., 2011a).

As a next step, we concentrated on deregulated genes encoding TF, as they are likely candidates for the observed differentiation block. The expression of a total of 1,620 genes encoding known TF was analyzed. 15 genes were identified whose expression was significantly up-regulated after RUNX1 inactivation in both AML samples, indicating that

their expression was repressed by RUNX1* (Fig. 7 C, left). These include key regulators of Meg/Ery differentiation (Doré and Crispino, 2011; Kaufmann et al., 2012; Pimkin et al., 2014). In addition, several genes whose expression is up-regulated during G/M differentiation were also suppressed by RUNX1* (Fig. S3). In contrast, loss of RUNX1 activity led to the down-regulation of only a few transcriptional regulators (Fig. 7 C, right), including several genes implicated in the control of cell cycle (*Myb* and *Mybbp1a*) or direct downstream regulators of proliferation stimulus (e.g., *Egr1*, *Mef2d*, and *Nop2*). Two genes (*Emx2* and *Hhex*) encoding homeotic box proteins belonging to the NK-like (NKL) subclass of *ANTP* homeobox genes were among the most strongly down-regulated genes after RUNX1 withdrawal.

HHEX is up-regulated in FLT3–ITD AML and by RUNX1 activation

Examination of AML patient databanks demonstrated that *EMX2* expression was extremely low in both FLT3-ITD^pos and FLT3-ITD^neg patient samples (not depicted), but *HHEX*
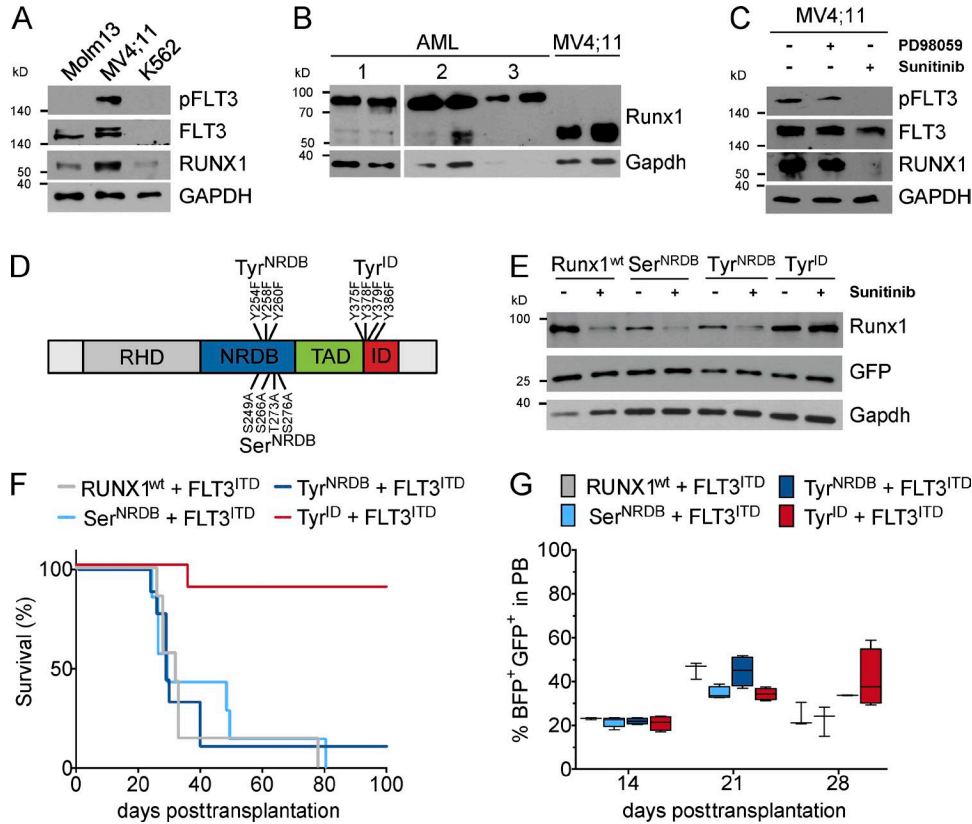
Figure 5. **RUNX1 requires posttranslational modification to execute its leukemogenic function.** (A) Western blot analysis of pFTL3 (Tyr591), FLT3, and RUNX1 proteins in Molm3 (FLT3-ITD[+]; not expressed), MV4;11 (FLT3-ITD[+]; expressed), and K562 (BCR-ABL) cells. (B) Western blot analysis of RUNX1 protein in three primary AML tumors (*B6.Runx1*[Δ/+] from independent experiments and in MV4;11 cells. Two independent extracts were loaded for each tumor cell. (C) Western blot analysis of pFTL3 (Tyr591), FLT3, and RUNX1 proteins in MV4;11 cells treated with either 40 µM PD98059 (MAPK inhibitor) or 1 µM Sunitinib (FLT3 inhibitor) for 24 h. The experiment was repeated twice with independent extracts. Two additional experiments were performed with 1 µM AC220, which confirmed reduced RUNX1 protein levels after 6-h treatment. (D) Schematic diagram of RUNX1, showing Tyr (Y)/serine (S)/threonine (T) residues mutated to generate RUNX1 phosphorylation mutants. NRDB, negative regulatory DNA binding; RHD, runt homology domain (DNA- and CBFβ-binding domain); TAD, trans-activating domain. (E) Western blot analysis of RUNX1 proteins in FDCP1 mouse progenitor cells transduced to express FLT3-ITD and RUNX1 phosphorylation mutants. Cells were cultured in medium containing 200 nM 4-OHT and treated with 500 nM Sunitinib as indicated for 24 h. GFP levels demonstrate similar transduction frequencies. (F) Kaplan-Meier survival curves of mice transplanted with *B6.Runx1*[Δ/+] HSPCs transduced with FLT3-ITD and the indicated RUNX1 phosphorylation mutant. Two independent infections and transplantations were performed with a total of eight mice per cohort. Double-positive transduction frequencies ranged from 1.8 to 3.8% for all constructs in both experiments. (G) Two-dimensional box plots showing mean (line), 25–75th percentiles (boxed), and SD (whiskers) of GFP[+]/BFP^{+} cells in the PB of three to five transplanted mice within each cohort at the indicated time points.

expression was high overall but with significantly higher expression observed in FLT3-ITD[pos] samples (Fig. 8 A). Thus, next, we determined whether the deregulation of the *Hhex* homeobox gene is directly mediated by RUNX1* and the importance of FLT3-ITD signaling in this deregulation. To confirm that *Hhex* is a direct target gene of Runx1, we interrogated Runx1 chromatin immunoprecipitation–binding data in G/M progenitor (GMP)–like FDC-P1 cells (Behrens et al., 2016) and hematopoietic stem cell (HSC)–like HPC7 cells (Wilson et al., 2010). Runx1-binding sites were observed in both HSC and GMP cell types and overlapped with binding sites for TFs specific for each cell type (e.g., Gfib or C/ebpα, respectively; Fig. 8 B). Next, we investigated whether

RUNX1* induction and/or suppression of FLT3-ITD activity influenced *Hhex* gene expression in mouse cells. A twofold increase in *Hhex* expression was observed upon RUNX1 activation, but inhibiting FLT3-ITD activity with Sunitinib blocked RUNX1-mediated *Hhex* stimulation (Fig. 8 C). Together, these results demonstrate that RUNX1 binds to and up-regulates expression of the *Hhex* gene and that the former activity is augmented by FLT3-ITD signaling.

Hhex together with FLT3–ITD induces AML in vivo

To determine whether Hhex (or Emx2) is a critical effector of AML induction in RUNX1*/FLT3-ITD AML, retroviral transduction/transplantation experiments were performed
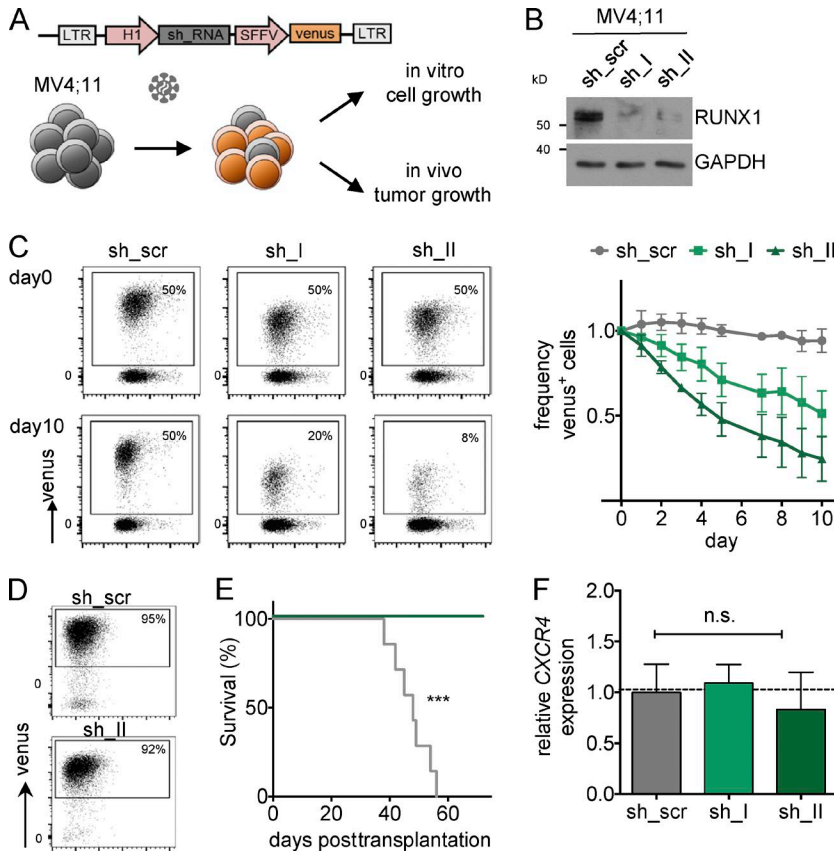
Figure 6. **High RUNX1 levels are required for transformation of human AML cells.** (A) Schematic representation of the experimental design is shown. FLT3-ITD–expressing MV4;11 cells were transduced with lentiviral vectors expressing RUNX1-specific or scrambled shRNA and analyzed for cell growth in vitro and tumor growth in vivo. SFFV, spleen focus-forming virus promoter. (B) Western blot analysis of RUNX1 in shRNA-transduced MV4;11 cells. (C) Representative flow cytometry analyses of shRNA-transduced and nontransduced MV4;11 in competitive in-vitro culture. The graph depicts the relative frequency of shRNA-transduced (Venus⁺) versus nontransduced cells over time. Shown is the mean of two independent experiments. Error bars represent SD. (D) Flow cytometry analyses of transduced MV4;11 cells before transplantation into NSG mice demonstrating efficient transduction of 95% (sh_scr) or 92% (RUNX1_sh_II). Two independent cell lines for each vector were established with similarly high transduction frequencies. (E) Combined Kaplan-Meier survival curves of the indicated NSG cohorts for two independent experiments with a total of seven mice per cohort. Mice were transplanted with 10^5 cells from two independently transduced MV4;11 cultures. The p-value was calculated by a Mantel-Cox log-rank test. ***, $P < 0.001$. (F) Relative transcript levels of *CXCR4* in scrambled or RUNX1-shRNA–transduced MV4;11 cells as determined by RT-PCR. $n = 3$. Error bars represent SD.

(Figs. 9, A and B). The analysis of PB of transduced mice at regular intervals demonstrated the loss of single transduced Venus⁺ (HHEX or Emx2) cells with time, but a notable selective advantage of double-positive HHEX/FLT3-ITD cells but not Emx2/FLT3-ITD cells was observed at week 6 (Fig. 9 C). AML developed in 90% of HHEX/FLT3-ITD mice with a median latency of 86 d (Fig. 9 D). Moribund mice presented with hepatosplenomegaly and leukocytosis (Fig. 9 E). The high invasiveness of the neoplastic cells was confirmed in sections of BM, liver, spleen, and lungs (Fig. 9 F and Fig. S4). Flow cytometry confirmed an outgrowth of Venus⁺/BFP⁺ cells in both BM and spleen, with the majority of cells in the Venus⁺/BFP⁺ population being CD11b⁺Gr1⁻, indicative of a myeloid progenitor, in contrast to normal CD11b⁺Gr1⁺ myeloid precursor and mature cells found in uninfected BM (Figs. 9, G and H). Examination of blood films confirmed the high levels of blasts and also granulocytic progenitors, typical of AML-M2 with granulocytic differentiation (Fig. 9 I). Furthermore, transplantation capacity of the neoplastic cells in conditioned recipients was confirmed (Fig. 9 J). These results demonstrate that RUNX1* and FLT3-ITD signaling impair differentiation in part by maintaining high HHEX expression levels.

DISCUSSION

Mutations that lead to constitutive activation of FLT3 are among the most common genetic events in AML and are strongly associated with poor prognosis. A characteristic feature of AML is a differentiation blockade at an early stage of development, and efforts to identify mechanisms to reverse this block have been a long-standing aim of leukemia research, stimulated by the success of differentiation therapy in the treatment of acute promyelocytic leukemia (Nowak et al., 2009; de Thé and Chen, 2010). Our results reveal a hitherto uncharacterized synergy between the RUNX1 TF and FLT3-ITD mutations in the induction of AML. Notably, our study shows that Tyr phosphorylation of RUNX1 is an essential molecular switch for this oncogenic synergy and that RUNX1 is a central mediator of a differentiation block that is partially mediated by up-regulating the *Hhex* homeobox gene (Fig. 10). The findings gained from our mouse model are also likely translatable to human AML. RUNX1 RNA levels are strongly enhanced in human AML patients carrying FLT3-ITD, and its downstream target *HHEX* is specifically up-regulated in FLT3-ITD human AML samples. Furthermore, human AML cells engineered to suppress RUNX1 expression lose leukemogenic activity.

An oncogenic role of RUNX1 in AML was somewhat unexpected because of its well established function as tumor suppressor in this disease. A high occurrence of inactivating mutations has been observed in AML (Osato et al., 1999; Schnittger et al., 2011), and analyses of conditional Runx1-deficient mice have demonstrated alterations in the
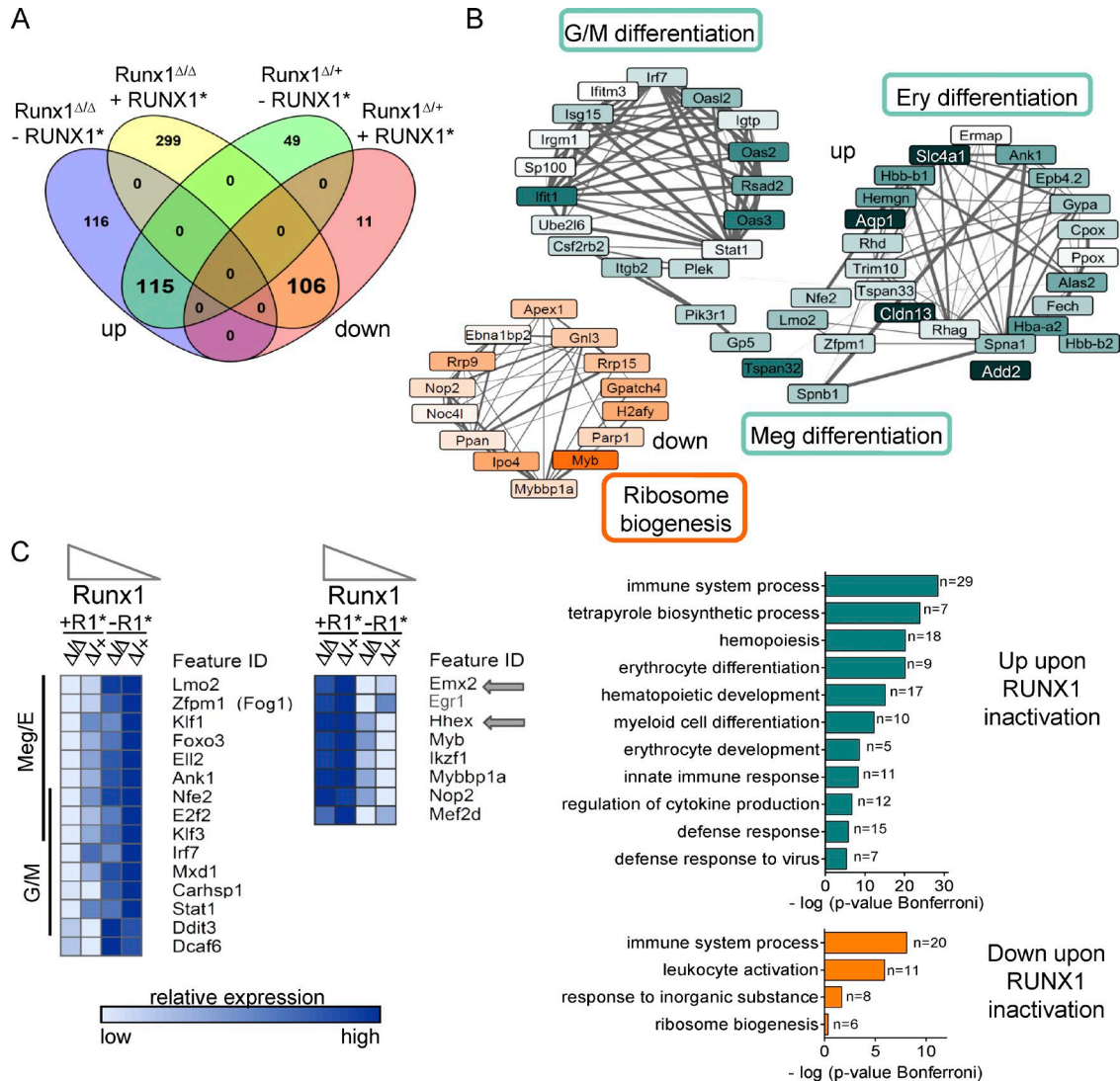
Figure 7. Identification of critical RUNX1 target genes in AML. (A) Four-way Venn diagram of genes with significant differential expression (greater than twofold with a Kal's z test false discovery rate P <0.05) between primary cultures with 4-OHT (+RUNX1*) or without (-RUNX1*) for two AML samples with either a *B6.Runx1*$^{\Delta/\Delta}$ or *B6.Runx1*$^{\Delta/+}$ genotype. Bold numbers denote the overlapping 115 genes that were up-regulated (green shade) and 106 genes down-regulated (orange shade) upon inactivation of RUNX1 in both samples. (B, top) Confidence view of protein interaction networks identified by analysis of the significantly up (orange)- or down (green)-regulated genes. Thicker lines represent stronger associations. Color intensity of the boxed genes denotes the relative difference in expression values, with darker shades representing greater differences. (Bottom) GO terms significantly enriched in up-regulated (green) and down-regulated (orange) gene sets are depicted. The number of deregulated genes for each GO term is indicated. (C) Significantly deregulated TF genes after inactivation of RUNX1 (−R*) as compared with activated RUNX1 (+R*) cultures. The *Runx1* genotype of the AML sample is indicated. A gradient of Runx1 activity level, as predicted from the presence/absence of 4-OHT and the *Runx1* genotype, is indicated and is reflected in the expression levels of the predicted RUNX1 target genes. TFs regulating Meg/Ery (Meg/E) and/or G/M differentiation are noted. Arrows denote the two NKL homeotic genes down-regulated after RUNX1 inactivation. See also Fig. S3.

self-renewal capacity of HSPCs, leading to an expansion of the myeloid progenitor compartment, particularly in those skewed toward Meg differentiation (Ross et al., 2012; Lam et al., 2014; Behrens et al., 2016)—all evidence supporting a tumor suppressor function. Our study also supports a tumor suppressor function in the initiation phase of leukemia development, as indicated by a shorter latency in Runx1-de-

ficient HSPCs. These results are supported by other studies that have demonstrated that Runx1-deficient cells show increased susceptibility to AML development (Jacob et al., 2010; Nishimoto et al., 2011). However, to our knowledge, this is the first study that demonstrates the dual tumor suppressor/oncogene function within the same cell system, although likely separated by temporal and spatial processes.
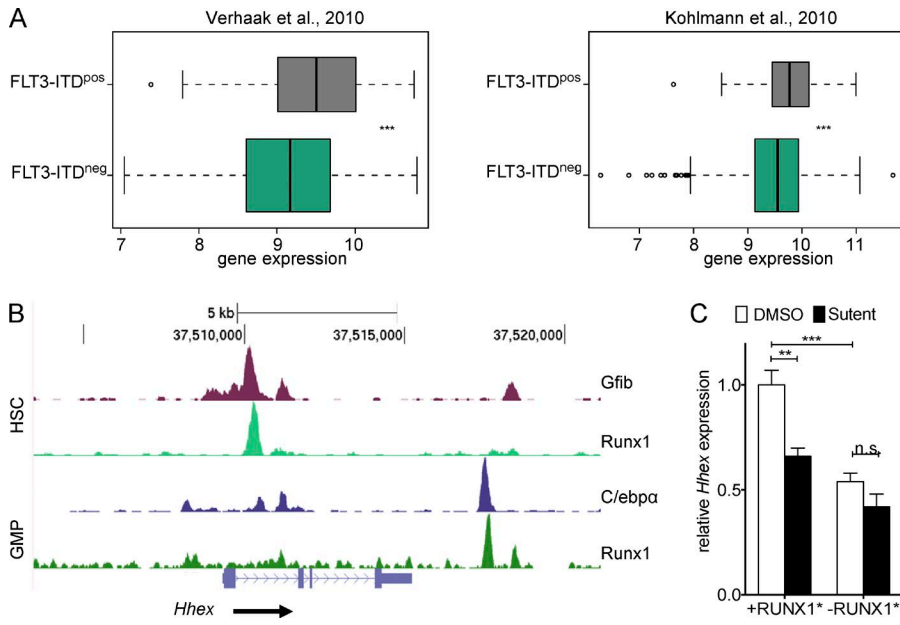
Figure 8. **HHEX is regulated by RUNX1 and FLT3–ITD signaling.** (A) *HHEX* expression (log2) of AML samples from two independent studies calculated using the Leukemia Gene Atlas. P-values were calculated by Welch's *t* test. ***, P < 0.001. (B) Density plots of Gfi1b (magenta) and Runx1 (light green) binding activity to the *Hhex* locus in HPC7 cells (Wilson et al., 2010) and of C/ebpα (blue; Hasemann et al., 2014) and Runx1 (green) in GMP cell lines (Behrens et al., 2016). Transcription direction (arrow) and exon–intron gene structure of the *Hhex* locus are depicted in a 5′-3′ orientation using the University of California, Santa Cruz Genome Browser (version mm9). (C) Relative transcript levels of *Hhex* in RUNX1-ERt2–expressing AML cells with (+RUNX1*) or without RUNX1 (−RUNX1*) activation and cultured in the presence or absence of Sunitinib (Sutent) for 22 h as determined by RT-PCR. Error bars represent SD of two independent experiments. **, P < 0.01; ***, P < 0.001.

RUNX1 oncogenic activity is partly attributable to the up-regulation of the *Hhex* gene encoding an NKL–homeotic protein. NKL and HOX-like proteins comprise the *antenna-pedia* class of homeobox proteins, which are transcriptional regulators involved in many key developmental processes including cell-fate decisions. Although the central role of HOX-like genes in developmental hematopoiesis and leukemia is well established (Rawat et al., 2012), the importance of NKL genes is just now being realized (Homminga et al., 2012). HHEX plays a critical role in lymphoid development and early T cell progenitor ALL (George et al., 2003; Homminga et al., 2011; Jackson et al., 2015), and recent work has also uncovered its essential role in MLL-induced myeloid leukemia (Shields et al., 2016). It is of interest to note that differentiation stage impacted by HHEX versus RUNX1 transformation differed in that whereas RUNX1 blocked both G/M and Meg/Ery differentiation pathways, only the former was blocked in HHEX/FLT3-ITD AML. Thus, it is likely that suppression of genes encoding Meg/Ery TFs (e.g., *LMO2*, *KLF1*, and *NFE2*) is also a key oncogenic function of RUNX1. Interestingly, the recent work of two groups collaborate with our findings that high RUNX1 expression levels are associated with FLT3-ITD AML and have identified several additional candidate target genes (Cauchy et al., 2015; Hirade et al., 2016). Our system offers a viable system to validate their causal importance.

Although our expression analysis favors the importance of a RUNX1-induced differentiation blockade in defining the oncogenic mechanism, its oncogenic potential is likely attributable to additional mechanisms. Notably, RUNX1 inactivation in AML cells led to the down-regulation of several genes associated with ribosome biogenesis, consistent with results from a recent study demonstrating Runx1 regulation

of this process in HSPCs (Cai et al., 2015). We postulate that activation of these genes by RUNX1 promotes sustained cell growth (Holland et al., 2004). However, we cannot rule out that up-regulation of genes involved in ribosome biogenesis reflects exit from the cell cycle through differentiation induction (Wong et al., 2011a). Interestingly, an oncogenic function of RUNX1 in mouse models of B and T cell lymphomas has been attributed to inhibiting p53 oncogene activity during stress response (Blyth et al., 2005; Kilbey et al., 2010). Furthermore, although the RUNX1 protein is not essential for myelopoiesis, recent studies have indicated that its expression is necessary and/or augments myeloid transformation by the RUNX1–RUNX1t1 and CBFβ/SMMHC (smooth muscle myosin heavy chain) fusion proteins (Ben-Ami et al., 2013; Goyama et al., 2013; Hyde et al., 2015; Mandoli et al., 2016). The ability of RUNX1 to inhibit apoptosis, either by up-regulation of Bcl2 or attenuation of the cell–cycle mitotic checkpoint, has been postulated to be the critical mechanism. Inhibiting apoptosis may contribute to the increased drug resistance observed in FLT3-ITD AML, which has recently been shown to correlate with RUNX1 expression (Hirade et al., 2016). Thus, RUNX1 likely exerts it oncogenic impact by a variety of overlapping mechanisms.

The unique association of FLT3-ITD mutations with AML as opposed to MPNs or myelodysplastic syndrome suggests a pivotal role in the differentiation block (Zheng and Small, 2005). Indeed, previous work has suggested that FLT3-ITD contributes to the block in myeloid differentiation through inhibiting the C/EBPα TF (Zheng and Small, 2005; Radomska et al., 2006). However, mouse models have demonstrated that *Cebpa* deficiency and FLT3-ITD expression are alone insufficient to induce AML (Reckzeh et al., 2012). An alternative or complimentary mechanism is sug-
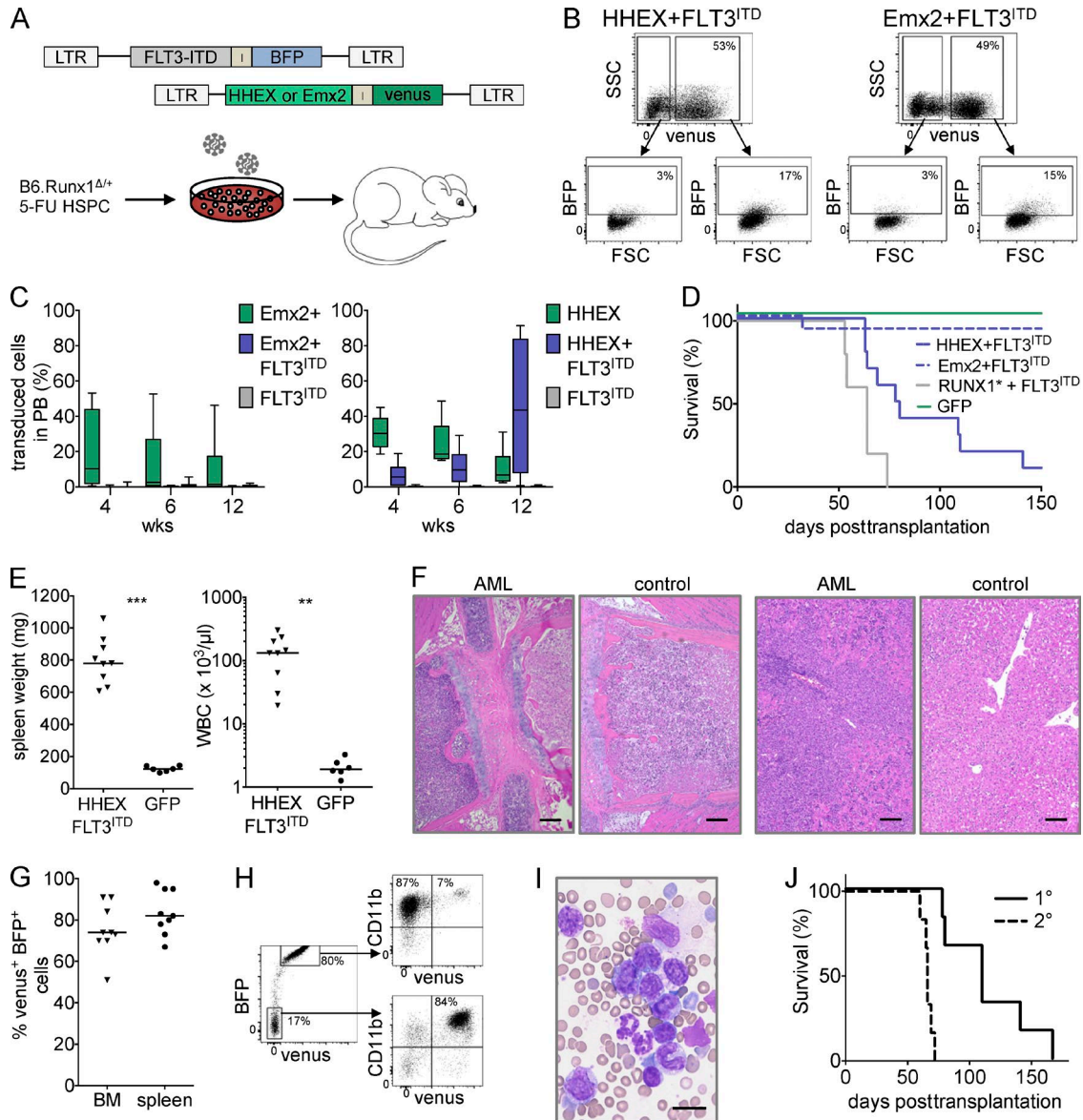
Figure 9. HHEX but not Emx2 cooperates with FLT3-ITD to induce AML. (A) Schematic representation of the experimental design is shown. HSPCs were isolated from BM cells of 5-FU–treated *B6.Runx1$^{\Delta/+}$*, cotransduced with the indicated retroviral vectors, and transplanted into conditioned recipient mice. (B) Representative flow cytometry plots of transduced HSPCs before transplantation demonstrating co-transduction (Venus$^+$/BFP$^+$) of HHEX/Venus (left) or Emx2/Venus (right) together with FLT3-ITD/BFP. Co-transduction frequencies of 15 and 5.3% for HHEX/FLT3-ITD and 17 and 16.3% for Emx2/FLT3-ITD were obtained in two independent experiments. FSC, forward scatter; SSC, side scatter. (C) Two-dimensional box plots showing the median (line), 25–75th percentiles (boxed), and SD (whiskers) of Venus$^+$/BFP$^+$ cells in the PB of transplanted mice (n = 10 per cohort) at the indicated time points. (D) Kaplan-Meier survival curves of mice receiving FLT3-ITD/BFP and either HHEX/Venus (n = 10) or Emx2/Venus (n = 13). As parallel positive and negative controls, cohorts receiving RUNX1-ER/FLT3-ITD and treated with 4-OHT (n = 6) or GFP alone (n = 6) were examined. (E) Spleen weight and leukocyte counts of either diseased (HHEX/FLT3-ITD; n = 9) or healthy negative-control GFP (n = 6) mice are plotted. Horizontal lines indicate median value for each cohort. P-values were calculated by a nonpaired Student's *t* test. **, P < 0.01; ***, P < 0.001. WBC, white blood cell. (F) Representative histological analysis of sections from sternum (left) and livers (right) from either an AML (HHEX/FLT3-ITD; n = 3) or control (GFP; n = 3) mouse. Expansion of leukemic cells in a single BM cavity is clearly observed, whereas the neighboring cavity is not impacted. Abundant and diffuse infiltrating hematopoietic cells (dark staining) were observed in the livers of AML mice leading to hepatomegaly. H&E staining was used. Bars, 300 µm. (G) Dot blot of double-positive (HHEX/Venus$^+$ and FLT3-ITD/BFP$^+$) cells in BM and spleen of diseased mice (n = 9) as determined by flow cytometry. Each dot represents the value for a single mouse. Horizontal lines indicate median value of all mice from two independent experiments. (H) Representative flow cytometry plots of dispersed BM cells from diseased mice demonstrating high levels of Venus$^+$/BFP$^+$ cells, which were consistently positive for CD11b alone (myeloid progenitor; mean 90 ± 3.9%; n = 7), as compared with normal myeloid precursors in the BM, which are double positive for both myeloid antigens (CD11b$^+$/Gr1$^+$; mean 88 ± 34.5%; n = 7). (I) Blood smears of mice demonstrating increased numbers of blasts and maturing cells in AML mice. Pappenheim stain was used. Bar, 20 µm. (J) Kaplan-Meier survival curves of serial transplantation of HHEX/FLT3-ITD$^+$ leukemic blasts in two independent experiments. n = 6 per transplantation.
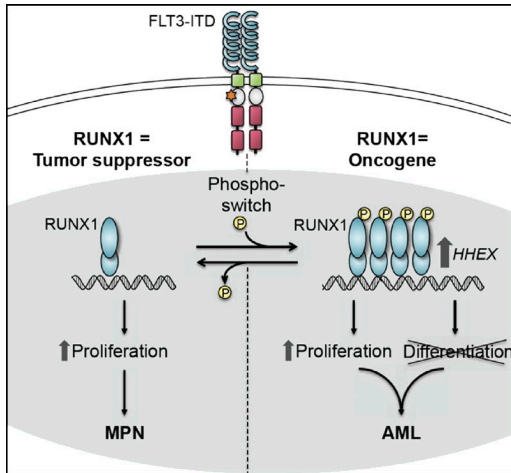
Figure 10. Graphical summary of the synergistic action of high levels of phosphorylated RUNX1 and FLT3–ITD signaling in AML. The depiction shows an important biological principle in acute leukemia in which cross talk between signaling pathways and transcriptional regulators act as a critical molecular switch to toggle a protein (e.g., RUNX1) between a tumor suppressor and a classical oncogene.

gested by our finding that RUNX1 protein levels are dependent on FLT3-ITD signaling in AML cells and that, together, they synergize to generate AML. High RUNX1 protein levels can be induced by several different mechanisms. Whereas our data support the hypothesis that FLT3 signaling impacts on protein levels via phosphorylation, the work of Cauchy et al. (2015) suggests that FLT3-ITD up-regulates *RUNX1* gene expression directly. Reconcilable with either mechanism is the hypothesis that high RUNX1 levels may also reflect a selective process during FLT3-ITD leukemogenesis, by which RUNX1-high–expressing clones become dominant because of the synergistic interplay of these two pathways.

Finally, our study underlines the important impact of RUNX1 phosphorylation on its oncogenic activity. Decisions of cell fate are clearly regulated by signaling pathways through posttranslational modifications of key TFs. Yet, deciphering the intricate posttranslational code and its ultimate impact on cellular processes has been challenging. Phosphorylation, in particular, is known to promote or inhibit protein–protein interactions and thereby act as a molecular switch between cell fates. It is well established that FLT3-ITD activates Src kinases (Choudhary et al., 2009; Leischner et al., 2012), and Src has been shown to alter the activity of Runx1 through phosphorylation, presumably through altered interactions with TF regulators and chromatin modulators (e.g., SWI/SNF [switch/sucrose nonfermentable]; Huang et al., 2012). Our work demonstrated that Tyr phosphorylation within the ID region of RUNX1 is critical for its oncogenic potential, and thus, an important next step will be to identify potential coregulatory proteins that bind to this domain. Significantly, previous studies have shown that Tyr phosphorylation impairs Meg and T cell development but increases Runx1 stability

and transactivation of *Cebpa* in myeloid cell lines (Huang et al., 2012; Leong et al., 2016).

The observation that inactivation of RUNX1 can promote differentiation of FLT3-ITD AML cells demonstrates that the leukemic stem cells have not acquired additional mutations that irrevocably alter their differentiation potential. These data suggest that therapies that can reverse this differentiation block will offer significant therapeutic efficacy in AML patients with FLT3-ITD mutations. This may include combination therapies that incorporate FLT3-ITD and Src inhibitors or small molecules that block RUNX1 phosphorylation or inhibit its function in regulating key target genes (Illendula et al., 2015). Considering the selective toxicity of Runx1 ablation to leukemic cells, but not to normal HSCs (Cai et al., 2011), inhibiting Runx1 may be a promising target for effective combination therapies in FLT3-ITD AML.

MATERIALS AND METHODS
Experimental animals
Littermates from B6.*Runx1*^{fl/+}-Tg(*vav*-Cre) X B6.*Runx1*^{fl/+} crosses were used for experiments (Behrens et al., 2016). B6.SJL-*Ptprc*[a]*Pec*[b]/BoyJ (B6-Ly.1) mice were used as hosts for BM transplantations. NOD.Cg-*Prkdc*[scid] *Il2rg*[tm1Wjl]/SzJ (NSG) mice were obtained from The Jackson Laboratory. All mice were maintained in a specific pathogen–free facility at the Heinrich-Pette-Institute animal facility. Animal experiments were approved by the Hamburg authorities and complied with the regulatory standards of the animal ethics committee.

HSPC transduction and transplantation
Standard mouse stem cell virus–based gamma-retroviral vectors were used to express (a) human RUNX1-ERt2 (Behrens et al., 2016), (b) human FLT3-ITD (Schmidt-Arras et al., 2005), and (c) human HHEX or mouse Emx2. Donor mice were injected with 150 mg/kg 5-fluoruracil (5-FU; Medac) 3 d before HSPC isolation. Transductions were performed as described previously (Schwieger et al., 2009). In brief, 3–5 × 10^5 HSPCs were co-transplanted with 5 × 10^4 spleen cells into lethally irradiated (9 Gy) B6-Ly.1 mice. RUNX1-ERt2 was induced in vivo at day 14 (pulse) or day 18 by administering tamoxifen citrate via standard food pellets (400 mg/kg; LASvendi LASCRDiets). For retransplantation assays, 5 × 10^6–10^7 tumor cells were injected in conditioned B6-Ly5.1 mice. In xenograft assays, 10^5 MV4;11 cells were intravenously transplanted into NSG mice.

Morphological and histological analysis of mice
Blood parameters were determined on a Hemavet 950 hematology system (Drew Scientific), and blood smears were stained according to the Pappenheim method (Sigma-Aldrich). Tissue samples of liver, lungs, and spleen were fixed in 4% (vol/vol) formalin and embedded in paraffin. Sterni were fixed in CALfix solution (Biocyc, Luckenwalde). Deparaffinized sections were stained with hematoxylin and eosin (H&E) or periodic acid Schiff solution (Sigma-Aldrich).

Cell culture

FDC-P1 (Dexter et al., 1980), MV4;11 (Quentmeier et al., 2003), and Molm 13 (Matsuo et al., 1997) cells were maintained as described previously. HSPCs and leukemic blasts were cultured in serum-free expansion media (StemSpan; STEMCELL Technologies) with 4 mM glutamine, 1 mM sodium pyruvate, 100 ng/ml mSCF, 100 ng/ml hIL-11, 100 ng/ml hFLT3L (PeproTech), and 10 ng/ml mIL-3 (Strathmann). RUNX1 activation was induced by culturing cells in 200 nM hydroxytamoxifen (Sigma-Aldrich). Inhibition of FLT3-ITD signaling was achieved by addition of Sunitinib (LC Laboratories) at the indicated concentration.

Cell purification and flow cytometry

For fluorescence-activated cell-sorter flow cytometry analysis and sorting, single-cell suspensions were prepared from blood, spleen, and BM. Erythrocytes were lysed (PharmLyse solution; BD), and cells were stained with fluorophore-conjugated antibodies (see Table S1 for list of antibodies) and analyzed or sorted on a FACS Canto II or Aria II (BD), respectively. Data acquisition and analysis were performed using FACS Diva software (BD).

Protein and RNA analyses

Proteins were extracted from cell pools with equal cell numbers using trichloroacetic acid and analyzed by Western blot analysis using standard procedures. See Table S2 for a list of antibodies used for analyses. For mRNA expression studies, total RNA was extracted using the peqGOLD TriFast kit (Peqlab). 1 µg RNA was used to generate cDNA libraries using TrueSeq RNA kits (Illumina). Sequencing was performed on a HiSeq 2500 sequencing system (Illumina). Reads were aligned to the mouse cDNA (genome browser version mm9; University of California, Santa Cruz), and reads per kilobase per million values were determined using the CLC_Genomic Workbench, with all parameters set to default settings. For illustration of deregulated genes, Venny 2.0.2 was used. Protein interaction network and enrichment analysis for GO terms (GO biological processes) were performed using STRING software (version 10; STRING Consortium). Networks were visualized using Cytoscape (version 3.2.0; Cytoscape Consortium). Heat maps were generated using GENE-E (version 3.0.204; Broad Institute). A comprehensive list of genes encoding TFs was obtained from the Riken Transcription Factor Database. RNA-Seq data from leukemic blasts have been deposited into the NCBI Gene Expression Omnibus portal under the accession no. GSE81422. For quantitative RT-PCR analysis, RNA was subjected to DNaseI digestion (Ambion) and converted to cDNA using avian myeloblastosis virus reverse transcriptase (New England Biolabs, Inc.). cDNA was used as a template for mRNA amplification by PowerSYBR Green PCR Master Mix (Roche; Applied Biosystems), run on a Light-Cycler 480 II system (Roche). Oligonucleotides are listed in Tables S3 and S4.

Online supplemental material

Figs. S1 and S4 contain additional histological results of diseased mice. Figs. S2 and S3 show heat maps of gene expression patterns in AML samples and normal hematopoiesis. Tables S1–S4 provide antibodies used for flow cytometry and Western blot analyses and oligo sequences for PCR and shRNA experiments.

REFERENCES

Behrens, K., I. Triviai, M. Schwieger, N. Tekin, M. Alawi, M. Spohn, D. Indenbirken, M. Ziegler, U. Müller, W.S. Alexander, and C. Stocking. 2016. Runx1 downregulates stem cell and megakaryocytic transcription programs that support niche interactions. *Blood.* 127:3369–3381. http://dx.doi.org/10.1182/blood-2015-09-668129

Ben-Ami, O., D. Friedman, D. Leshkowitz, D. Goldenberg, K. Orlovsky, N. Pencovich, J. Lotem, A. Tanay, and Y. Groner. 2013. Addiction of t(8;21) and inv(16) acute myeloid leukemia to native RUNX1. *Cell Reports.* 4:1131–1143. http://dx.doi.org/10.1016/j.celrep.2013.08.020

Blyth, K., E.R. Cameron, and J.C. Neil. 2005. The RUNX genes: gain or loss of function in cancer. *Nat. Rev. Cancer.* 5:376–387. http://dx.doi.org/10.1038/nrc1607

Burnett, A., M. Wetzler, and B. Löwenberg. 2011. Therapeutic advances in acute myeloid leukemia. *J. Clin. Oncol.* 29:487–494. http://dx.doi.org/10.1200/JCO.2010.30.1820

Cai, X., J.J. Gaudet, J.K. Mangan, M.J. Chen, M.E. De Obaldia, Z. Oo, P. Ernst, and N.A. Speck. 2011. Runx1 loss minimally impacts long-term hematopoietic stem cells. *PLoS One.* 6:e28430. http://dx.doi.org/10.1371/journal.pone.0028430

Cai, X., L. Gao, L. Teng, J. Ge, Z.M. Oo, A.R. Kumar, D.G. Gilliland, P.J. Mason, K. Tan, and N.A. Speck. 2015. Runx1 deficiency decreases ribosome biogenesis and confers stress resistance to hematopoietic stem and progenitor cells. *Cell Stem Cell.* 17:165–177. http://dx.doi.org/10.1016/j.stem.2015.06.002

Cancer Genome Atlas Research Network. 2013. Genomic and epigenomic landscapes of adult de novo acute myeloid leukemia. *N. Engl. J. Med.* 368:2059–2074. http://dx.doi.org/10.1056/NEJMoa1301689

Cauchy, P., S.R. James, J. Zacarias-Cabeza, A. Ptasinska, M.R. Imperato, S.A. Assi, J. Piper, M. Canestraro, M. Hoogenkamp, M. Raghavan, et al. 2015. Chronic FLT3-ITD signaling in acute myeloid leukemia is connected to a specific chromatin signature. *Cell Reports.* 12:821–836. http://dx.doi.org/10.1016/j.celrep.2015.06.069

Challen, G.A., and M.A. Goodell. 2010. Runx1 isoforms show differential expression patterns during hematopoietic development but have similar functional effects in adult hematopoietic stem cells. *Exp. Hematol.* 38:403–416. http://dx.doi.org/10.1016/j.exphem.2010.02.011

Choudhary, C., J.V. Olsen, C. Brandts, J. Cox, P.N. Reddy, F.D. Böhmer, V. Gerke, D.-E.E. Schmidt-Arras, W.E. Berdel, C. Müller-Tidow, et al. 2009. Mislocalized activation of oncogenic RTKs switches downstream signaling outcomes. *Mol. Cell.* 36:326–339. http://dx.doi.org/10.1016/j.molcel.2009.09.019

Chu, S.H., D. Heiser, L. Li, I. Kaplan, M. Collector, D. Huso, S.J. Sharkis, C. Civin, and D. Small. 2012. FLT3-ITD knockin impairs hematopoietic stem cell quiescence/homeostasis, leading to myeloproliferative neoplasm. *Cell Stem Cell.* 11:346–358. http://dx.doi.org/10.1016/j.stem.2012.05.027

Collins, A., D.R. Littman, and I. Taniuchi. 2009. RUNX proteins in transcription factor networks that regulate T-cell lineage choice. *Nat. Rev. Immunol.* 9:106–115. http://dx.doi.org/10.1038/nri2489

de Thé, H., and Z. Chen. 2010. Acute promyelocytic leukaemia: novel insights into the mechanisms of cure. *Nat. Rev. Cancer.* 10:775–783. http://dx.doi.org/10.1038/nrc2943

Dexter, T.M., J. Garland, D. Scott, E. Scolnick, and D. Metcalf. 1980. Growth of factor-dependent hemopoietic precursor cell lines. *J. Exp. Med.* 152:1036–1047. http://dx.doi.org/10.1084/jem.152.4.1036

Doré, L.C., and J.D. Crispino. 2011. Transcription factor networks in erythroid cell and megakaryocyte development. *Blood.* 118:231–239. http://dx.doi.org/10.1182/blood-2011-04-285981

Gale, R.E., C. Green, C. Allen, A.J. Mead, A.K. Burnett, R.K. Hills, and D.C. Linch. Medical Research Council Adult Leukaemia Working Party. 2008. The impact of FLT3 internal tandem duplication mutant level, number, size, and interaction with NPM1 mutations in a large cohort of young adult patients with acute myeloid leukemia. *Blood.* 111:2776–2784. http://dx.doi.org/10.1182/blood-2007-08-109090

Genovese, G., A.K. Kähler, R.E. Handsaker, J. Lindberg, S.A. Rose, S.F. Bakhoum, K. Chambert, E. Mick, B.M. Neale, M. Fromer, et al. 2014. Clonal hematopoiesis and blood-cancer risk inferred from blood DNA sequence. *N. Engl. J. Med.* 371:2477–2487. http://dx.doi.org/10.1056/NEJMoa1409405

George, A., H.C. Morse III, and M.J. Justice. 2003. The homeobox gene *Hex* induces T-cell-derived lymphomas when overexpressed in hematopoietic precursor cells. *Oncogene.* 22:6764–6773. http://dx.doi.org/10.1038/sj.onc.1206822

Goyama, S., J. Schibler, L. Cunningham, Y. Zhang, Y. Rao, N. Nishimoto, M. Nakagawa, A. Olsson, M. Wunderlich, K.A. Link, et al. 2013. Transcription factor RUNX1 promotes survival of acute myeloid leukemia cells. *J. Clin. Invest.* 123:3876–3888. http://dx.doi.org/10.1172/JCI68557

Goyama, S., G. Huang, M. Kurokawa, and J. Mulloy. 2015. Posttranslational modifications of RUNX1 as potential anticancer targets. *Oncogene.* 34:3483–3492. http://dx.doi.org/10.1038/onc.2014.305

Grossmann, V., W. Kern, S. Harbich, T. Alpermann, S. Jeromin, S. Schnittger, C. Haferlach, T. Haferlach, and A. Kohlmann. 2011. Prognostic relevance of RUNX1 mutations in T-cell acute lymphoblastic leukemia. *Haematologica.* 96:1874–1877. http://dx.doi.org/10.3324/haematol.2011.043919

Growney, J.D., H. Shigematsu, Z. Li, B.H. Lee, J. Adelsperger, R. Rowan, D.P. Curley, J.L. Kutok, K. Akashi, I.R. Williams, et al. 2005. Loss of Runx1 perturbs adult hematopoiesis and is associated with a myeloproliferative phenotype. *Blood.* 106:494–504. http://dx.doi.org/10.1182/blood-2004-08-3280

Grundler, R., C. Miething, C. Thiede, C. Peschel, and J. Duyster. 2005. FLT3-ITD and tyrosine kinase domain mutants induce 2 distinct phenotypes in a murine bone marrow transplantation model. *Blood.* 105:4792–4799. http://dx.doi.org/10.1182/blood-2004-11-4430

Hasemann, M.S., F.K. Lauridsen, J. Waage, J.S. Jakobsen, A.-K.K. Frank, M.B. Schuster, N. Rapin, F.O. Bagger, P.S. Hoppe, T. Schroeder, and B.T. Porse. 2014. C/EBPα is required for long-term self-renewal and lineage priming of hematopoietic stem cells and for the maintenance of epigenetic configurations in multipotent progenitors. *PLoS Genet.* 10:e1004079. http://dx.doi.org/10.1371/journal.pgen.1004079

Hebestreit, K., S. Gröttrup, D. Emden, J. Veerkamp, C. Ruckert, H.U. Klein, C. Müller-Tidow, and M. Dugas. 2012. Leukemia gene atlas—a public platform for integrative exploration of genome-wide molecular data. *PLoS One.* 7:e39148. http://dx.doi.org/10.1371/journal.pone.0039148

Hirade, T., M. Abe, C. Onishi, T. Taketani, S. Yamaguchi, and S. Fukuda. 2016. Internal tandem duplication of FLT3 deregulates proliferation and differentiation and confers resistance to the FLT3 inhibitor AC220 by up-regulating RUNX1 expression in hematopoietic cells. *Int. J. Hematol.* 103:95–106. http://dx.doi.org/10.1007/s12185-015-1908-8

Holland, E.C., N. Sonenberg, P.P. Pandolfi, and G. Thomas. 2004. Signaling control of mRNA translation in cancer pathogenesis. *Oncogene.* 23:3138–3144. http://dx.doi.org/10.1038/sj.onc.1207590

Homminga, I., R. Pieters, A.W. Langerak, J.J. de Rooi, A. Stubbs, M. Verstegen, M. Vuerhard, J. Buijs-Gladdines, C. Kooi, P. Klous, et al. 2011. Integrated transcript and genome analyses reveal NKX2-1 and MEF2C as potential oncogenes in T cell acute lymphoblastic leukemia. *Cancer Cell.* 19:484–497. http://dx.doi.org/10.1016/j.ccr.2011.02.008

Homminga, I., R. Pieters, and J.P. Meijerink. 2012. NKL homeobox genes in leukemia. *Leukemia.* 26:572–581. http://dx.doi.org/10.1038/leu.2011.330

Huang, H., A.J. Woo, Z. Waldon, Y. Schindler, T.B. Moran, H.H. Zhu, G.-S.S. Feng, H. Steen, and A.B. Cantor. 2012. A Src family kinase–Shp2 axis controls RUNX1 activity in megakaryocyte and T-lymphocyte differentiation. *Genes Dev.* 26:1587–1601. http://dx.doi.org/10.1101/gad.192054.112

Hyde, R.K., L. Zhao, L. Alemu, and P.P. Liu. 2015. Runx1 is required for hematopoietic defects and leukemogenesis in Cbfb-MYH11 knock-in mice. *Leukemia.* 29:1771–1778. http://dx.doi.org/10.1038/leu.2015.58

Ichikawa, M., T. Asai, T. Saito, S. Seo, I. Yamazaki, T. Yamagata, K. Mitani, S. Chiba, S. Ogawa, M. Kurokawa, and H. Hirai. 2004. AML-1 is required for megakaryocytic maturation and lymphocytic differentiation, but not for maintenance of hematopoietic stem cells in adult hematopoiesis. *Nat. Med.* 10:299–304. http://dx.doi.org/10.1038/nm997

Illendula, A., J.A. Pulikkan, H. Zong, J. Grembecka, L. Xue, S. Sen, Y. Zhou, A. Boulton, A. Kuntimaddi, Y. Gao, et al. 2015. A small-molecule inhibitor of the aberrant transcription factor CBFβ-SMMHC delays leukemia in mice. *Science.* 347:779–784. http://dx.doi.org/10.1126/science.aaa0314

Jackson, J.T., C. Nasa, W. Shi, N.D. Huntington, C.W. Bogue, W.S. Alexander, and M.P. McCormack. 2015. A crucial role for the homeodomain transcription factor Hhex in lymphopoiesis. *Blood.* 125:803–814. http://dx.doi.org/10.1182/blood-2014-06-579813

Jacob, B., M. Osato, N. Yamashita, C.Q. Wang, I. Taniuchi, D.R. Littman, N. Asou, and Y. Ito. 2010. Stem cell exhaustion due to Runx1 deficiency is prevented by Evi5 activation in leukemogenesis. *Blood.* 115:1610–1620. http://dx.doi.org/10.1182/blood-2009-07-232249

Kaufmann, K.B., A. Gründer, T. Hadlich, J. Wehrle, M. Gothwal, R. Bogeska, T.S. Seeger, S. Kayser, K.-B. Pham, J.S. Jutzi, et al. 2012. A novel murine model of myeloproliferative disorders generated by overexpression of the transcription factor NF-E2. *J. Exp. Med.* 209:35–50. http://dx.doi.org/10.1084/jem.20110540

Kilbey, A., A. Terry, A. Jenkins, G. Borland, Q. Zhang, M.J. Wakelam, E.R. Cameron, and J.C. Neil. 2010. Runx regulation of sphingolipid metabolism and survival signaling. *Cancer Res.* 70:5860–5869. http://dx.doi.org/10.1158/0008-5472.CAN-10-0726

Kohlmann, A., L. Bullinger, C. Thiede, M. Schaich, S. Schnittger, K. Döhner, M. Dugas, H.U. Klein, H. Döhner, G. Ehninger, and T. Haferlach. 2010. Gene expression profiling in AML with normal karyotype can predict mutations for molecular markers and allows novel insights into

perturbed biological pathways. *Leukemia*. 24:1216–1220. http://dx.doi .org/10.1038/leu.2010.73

Lam, K., and D.-E. Zhang. 2012. RUNX1 and RUNX1-ETO: roles in hematopoiesis and leukemogenesis. *Front. Biosci. (Landmark Ed.)*. 17:1120–1139. http://dx.doi.org/10.2741/3977

Lam, K., A. Muselman, R. Du, Y. Harada, A.G. Scholl, M. Yan, S. Matsuura, S. Weng, H. Harada, and D.-E. Zhang. 2014. Hmga2 is a direct target gene of RUNX1 and regulates expansion of myeloid progenitors in mice. *Blood*. 124:2203–2212. http://dx.doi.org/10.1182/blood-2014 -02-554543

Lee, B.H., Z. Tothova, R.L. Levine, K. Anderson, N. Buza-Vidas, D.E. Cullen, E.P. McDowell, J. Adelsperger, S. Fröhling, B.J. Huntly, et al. 2007. FLT3 mutations confer enhanced proliferation and survival properties to multipotent progenitors in a murine model of chronic myelomonocytic leukemia. *Cancer Cell*. 12:367–380. http://dx.doi.org/10.1016/j.ccr .2007.08.031

Leischner, H., C. Albers, R. Grundler, E. Razumovskaya, K. Spiekermann, S. Bohlander, L. Rönnstrand, K. Götze, C. Peschel, and J. Duyster. 2012. SRC is a signaling mediator in FLT3-ITD- but not in FLT3-TKD-positive AML. *Blood*. 119:4026–4033. http://dx.doi.org/10.1182/blood -2011-07-365726

Leong, W.Y., H. Guo, O. Ma, H. Huang, A.B. Cantor, and A.D. Friedman. 2016. Runx1 phosphorylation by Src increases trans-activation via augmented stability, reduced histone deacetylase (HDAC) binding, and increased DNA affinity, and activated Runx1 favors granulopoiesis. *J. Biol. Chem*. 291:826–836. http://dx.doi.org/10.1074/jbc.M115.674234

Mandoli, A., A.A. Singh, K.H. Prange, E. Tijchon, M. Oerlemans, R. Dirks, M. Ter Huurne, A.T. Wierenga, E.M. Janssen-Megens, K. Berentsen, et al. 2016. The hematopoietic transcription factors RUNX1 and ERG prevent AML1–ETO oncogene overexpression and onset of the apoptosis program in t(8;21) AMLs. *Cell Reports*. 17:2087–2100. http:// dx.doi.org/10.1016/j.celrep.2016.08.082

Marcucci, G., T. Haferlach, and H. Döhner. 2011. Molecular genetics of adult acute myeloid leukemia: prognostic and therapeutic implications. *J. Clin. Oncol*. 29:475–486. http://dx.doi.org/10.1200/JCO.2010.30.2554

Matsuo, Y., R.A. MacLeod, C.C. Uphoff, H.G. Drexler, C. Nishizaki, Y. Katayama, G. Kimura, N. Fujii, E. Omoto, M. Harada, and K. Orita. 1997. Two acute monocytic leukemia (AML-M5a) cell lines (MOLM-13 and MOLM-14) with interclonal phenotypic heterogeneity showing *MLL-AF9* fusion resulting from an occult chromosome insertion, ins(11;9)(q23;p22p23). *Leukemia*. 11:1469–1477. http://dx.doi.org/10 .1038/sj.leu.2400768

Niebuhr, B., M. Fischer, M. Täger, J. Cammenga, and C. Stocking. 2008. Gatekeeper function of the RUNX1 transcription factor in acute leukemia. *Blood Cells Mol. Dis*. 40:211–218. http://dx.doi.org/10.1016 /j.bcmd.2007.07.018

Niebuhr, B., N. Kriebitzsch, M. Fischer, K. Behrens, T. Günther, M. Alawi, U. Bergholz, U. Müller, S. Roscher, M. Ziegler, et al. 2013. Runx1 is essential at two stages of early murine B-cell development. *Blood*. 122:413–423. http://dx.doi.org/10.1182/blood-2013-01-480244

Nishimoto, N., S. Arai, M. Ichikawa, M. Nakagawa, S. Goyama, K. Kumano, T. Takahashi, Y. Kamikubo, Y. Imai, and M. Kurokawa. 2011. Loss of AML1/ Runx1 accelerates the development of MLL-ENL leukemia through down-regulation of p19ARF. *Blood*. 118:2541–2550. http://dx.doi.org /10.1182/blood-2010-10-315440

Nowak, D., D. Stewart, and H.P. Koeffler. 2009. Differentiation therapy of leukemia: 3 decades of development. *Blood*. 113:3655–3665. http://dx .doi.org/10.1182/blood-2009-01-198911

Osato, M., N. Asou, E. Abdalla, K. Hoshino, H. Yamasaki, T. Okubo, H. Suzushima, K. Takatsuki, T. Kanno, K. Shigesada, and Y. Ito. 1999. Biallelic and heterozygous point mutations in the runt domain of the *AML1/PEBP2αB* gene associated with myeloblastic leukemias. *Blood*. 93:1817–1824.

Paguirigan, A.L., J. Smith, S. Meshinchi, M. Carroll, C. Maley, and J.P. Radich. 2015. Single-cell genotyping demonstrates complex clonal diversity in acute myeloid leukemia. *Sci. Transl. Med*. 7:281re2. http://dx.doi.org/10 .1126/scitranslmed.aaa0763

Patel, J.P., M. Gönen, M.E. Figueroa, H. Fernandez, Z. Sun, J. Racevskis, P. Van Vlierberghe, I. Dolgalev, S. Thomas, O. Aminova, et al. 2012. Prognostic relevance of integrated genetic profiling in acute myeloid leukemia. *N. Engl. J. Med*. 366:1079–1089. http://dx.doi.org/10.1056/ NEJMoa1112304

Pimkin, M., A.V. Kossenkov, T. Mishra, C.S. Morrissey, W. Wu, C.A. Keller, G.A. Blobel, D. Lee, M.A. Beer, R.C. Hardison, and M.J. Weiss. 2014. Divergent functions of hematopoietic transcription factors in lineage priming and differentiation during erythro-megakaryopoiesis. *Genome Res*. 24:1932–1944. http://dx.doi.org/10.1101/gr.164178.113

Quentmeier, H., J. Reinhardt, M. Zaborski, and H.G. Drexler. 2003. FLT3 mutations in acute myeloid leukemia cell lines. *Leukemia*. 17:120–124. http://dx.doi.org/10.1038/sj.leu.2402740

Radomska, H.S., D.S. Bassères, R. Zheng, P. Zhang, T. Dayaram, Y. Yamamoto, D.W. Sternberg, N. Lokker, N.A. Giese, S.K. Bohlander, et al. 2006. Block of C/EBPα function by phosphorylation in acute myeloid leukemia with FLT3 activating mutations. *J. Exp. Med*. 203:371–381. http://dx .doi.org/10.1084/jem.20052242

Rawat, V.P., R.K. Humphries, and C. Buske. 2012. Beyond Hox: the role of ParaHox genes in normal and malignant hematopoiesis. *Blood*. 120:519– 527. http://dx.doi.org/10.1182/blood-2012-02-385898

Reckzeh, K., O. Bereshchenko, A. Mead, M. Rehn, S. Kharazi, S.E. Jacobsen, C. Nerlov, and J. Cammenga. 2012. Molecular and cellular effects of oncogene cooperation in a genetically accurate AML mouse model. *Leukemia*. 26:1527–1536. http://dx.doi.org/10.1038/leu.2012.37

Rosenbauer, F., and D.G. Tenen. 2007. Transcription factors in myeloid development: balancing differentiation with transformation. *Nat. Rev. Immunol*. 7:105–117. http://dx.doi.org/10.1038/nri2024

Ross, K., A.K. Sedello, G.P. Todd, M. Paszkowski-Rogacz, A.W. Bird, L. Ding, T. Grinenko, K. Behrens, N. Hubner, M. Mann, et al. 2012. Polycomb group ring finger 1 cooperates with Runx1 in regulating differentiation and self-renewal of hematopoietic cells. *Blood*. 119:4152–4161. http:// dx.doi.org/10.1182/blood-2011-09-382390

Sanders, M.A., and P.J.M. Valk. 2013. The evolving molecular genetic landscape in acute myeloid leukaemia. *Curr. Opin. Hematol*. 20:79–85. http://dx.doi.org/10.1097/MOH.0b013e32835d821c

Schmidt-Arras, D.E., A. Böhmer, B. Markova, C. Choudhary, H. Serve, and F.D. Böhmer. 2005. Tyrosine phosphorylation regulates maturation of receptor tyrosine kinases. *Mol. Cell. Biol*. 25:3690–3703. http://dx.doi .org/10.1128/MCB.25.9.3690-3703.2005

Schnittger, S., F. Dicker, W. Kern, N. Wendland, J. Sundermann, T. Alpermann, C. Haferlach, and T. Haferlach. 2011. RUNX1 mutations are frequent in de novo AML with noncomplex karyotype and confer an unfavorable prognosis. *Blood*. 117:2348–2357. http://dx.doi.org/10.1182/blood -2009-11-255976

Schwieger, M., A. Schüler, M. Forster, A. Engelmann, M.A. Arnold, R. Delwel, P.J. Valk, J. Löhler, R.K. Slany, E.N. Olson, and C. Stocking. 2009. Homing and invasiveness of MLL/ENL leukemic cells is regulated by MEF2C. *Blood*. 114:2476–2488. http://dx.doi.org/10.1182/blood -2008-05-158196

Shields, B.J., J.T. Jackson, D. Metcalf, W. Shi, Q. Huang, A.L. Garnham, S.P. Glaser, D. Beck, J.E. Pimanda, C.W. Bogue, et al. 2016. Acute myeloid leukemia requires Hhex to enable PRC2-mediated epigenetic repression of *Cdkn2a*. *Genes Dev*. 30:78–91. http://dx.doi.org/10.1101 /gad.268425.115

Shlush, L.I., S. Zandi, A. Mitchell, W.C. Chen, J.M. Brandwein, V. Gupta, J.A. Kennedy, A.D. Schimmer, A.C. Schuh, K.W. Yee, et al. HALT Pan-Leukemia Gene Panel Consortium. 2014. Identification of pre-leukaemic

haematopoietic stem cells in acute leukaemia. *Nature.* 506:328–333. http://dx.doi.org/10.1038/nature13038

Small, D. 2006. FLT3 mutations: biology and treatment. *Hematology (Am Soc Hematol Educ Program).* 2006:178–184.

Stirewalt, D.L., and J.P. Radich. 2003. The role of FLT3 in haematopoietic malignancies. *Nat. Rev. Cancer.* 3:650–665. http://dx.doi.org/10.1038/nrc1169

Thiede, C., C. Steudel, B. Mohr, M. Schaich, U. Schäkel, U. Platzbecker, M. Wermke, M. Bornhäuser, M. Ritter, A. Neubauer, et al. 2002. Analysis of FLT3-activating mutations in 979 patients with acute myelogenous leukemia: association with FAB subtypes and identification of subgroups with poor prognosis. *Blood.* 99:4326–4335. http://dx.doi.org/10.1182/blood.V99.12.4326

Verhaak, R.G., B.J. Wouters, C.A. Erpelinck, S. Abbas, H.B. Beverloo, S. Lugthart, B. Löwenberg, R. Delwel, and P.J. Valk. 2009. Prediction of molecular subtypes in acute myeloid leukemia based on gene expression profiling. *Haematologica.* 94:131–134. http://dx.doi.org/10.3324/haematol.13299

Welch, J.S., T.J. Ley, D.C. Link, C.A. Miller, D.E. Larson, D.C. Koboldt, L.D. Wartman, T.L. Lamprecht, F. Liu, J. Xia, et al. 2012. The origin and evolution of mutations in acute myeloid leukemia. *Cell.* 150:264–278. http://dx.doi.org/10.1016/j.cell.2012.06.023

Wilson, N.K., S.D. Foster, X. Wang, K. Knezevic, J. Schütte, P. Kaimakis, P.M. Chilarska, S. Kinston, W.H. Ouwehand, E. Dzierzak, et al. 2010. Combinatorial transcriptional control in blood stem/progenitor cells: genome-wide analysis of ten major transcriptional regulators. *Cell Stem Cell.* 7:532–544. http://dx.doi.org/10.1016/j.stem.2010.07.016

Wong, P., S.M. Hattangadi, A.W. Cheng, G.M. Frampton, R.A. Young, and H.F. Lodish. 2011a. Gene induction and repression during terminal erythropoiesis are mediated by distinct epigenetic changes. *Blood.* 118:e128–e138. http://dx.doi.org/10.1182/blood-2011-03-341404

Wong, W.F., K. Kohu, T. Chiba, T. Sato, and M. Satake. 2011b. Interplay of transcription factors in T-cell differentiation and function: the role of Runx. *Immunology.* 132:157–164. http://dx.doi.org/10.1111/j.1365-2567.2010.03381.x

Zheng, R., and D. Small. 2005. Mutant FLT3 signaling contributes to a block in myeloid differentiation. *Leuk. Lymphoma.* 46:1679–1687. http://dx.doi.org/10.1080/10428190500261740